PPV–PAMAM Hybrid Dendrimers: Self-Assembly and Stabilization of Gold Nanoparticles

ARTICLE *in* MACROMOLECULES · SEPTEMBER 2013

Impact Factor: 5.8 · DOI: 10.1021/ma401505k

Macromolecules

Article

pubs.acs.org/Macromolecules

PPV–PAMAM Hybrid Dendrimers: Self-Assembly and Stabilization of Gold Nanoparticles

Javier Guerra,[†,∥] Ana C. Rodrigo,[†,∥] Sonia Merino,[†] Juan Tejeda,[†] Joaquín C. García-Martínez,[‡] Prado Sánchez-Verdú,[†] Valentín Ceña,[§] and Julián Rodríguez-López*[,†]

[†]Área de Química Orgánica, Facultad de Ciencias y Tecnologías Químicas, Universidad de Castilla-La Mancha, 13071 Ciudad Real, Spain

[‡]Química Orgánica Farmacéutica, Facultad de Farmacia, Universidad de Castilla-La Mancha, 02071 Albacete, Spain

[§]Unidad Asociada Neurodeath, Facultad de Medicina, CSIC-Universidad de Castilla-La Mancha, 02006 Albacete, Spain, and CIBERNED, Instituto de Salud Carlos III, 28071 Madrid, Spain

Supporting Information

ABSTRACT: Different generations of PPV–PAMAM hybrid dendrimers have been prepared and characterized. Our initial studies showed the high tendency of these materials to aggregate and form nanoassemblies in different media. Nile Red experiments and DLS measurements allowed us to determine the critical aggregation concentration (CAC) and the size of the aggregates, which have also been used to stabilize small gold nanoparticles. The nanoparticles influence the assembly and optical properties of the dendrimer molecules and lead to strong quenching of their intrinsic fluorescence. Nevertheless, these gold particles will be very useful as biomarkers in living cells by means of electron microscopy because of their high electron contrast.

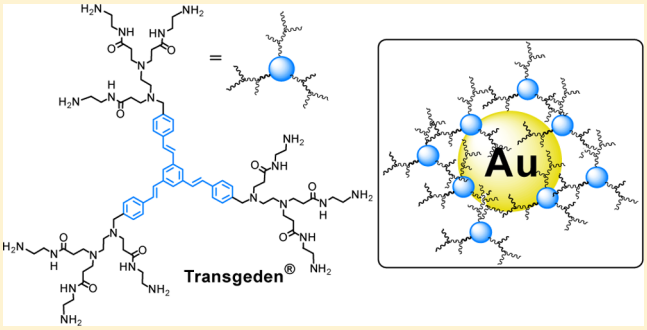

INTRODUCTION

Nanoparticles play an important role in drug delivery (chemotherapy) and in the delivery of biological therapies, which include gene therapy, vaccines, RNA interference, and antisense therapeutics.[1] A diverse range of targeted nanoparticles capable of delivering therapeutic and diagnostic agents to specific biological targets have been developed. These include an increasing number of nanoscale vehicles with distinct physicochemical and biological properties. Besides liposomes and polymeric conjugates, the most commonly used nanoparticle platforms are quantum dots, carbon nanotubes, metal nanoparticles (especially gold nanoparticles), dendrimers, and nanoassemblies or nanocomposites as nanoparticle-based platforms.[2] Among them, dendrimers have emerged as a novel class of nanoparticle platform because of their unique features such as monodispersity, multivalent properties, and well-defined architectures derived from synthetic control and design.[3] For these reasons an increasing number of research groups are choosing dendrimers for their gene and drug delivery experiments, and these are mainly poly(amidoamine), poly(propyleneimine), and polylysine dendrimers.[4] In this context, the excellent results obtained by different research groups working with amphiphilic dendrimers are remarkable.[5] In 2011, we reported the synthesis of a poly(phenylenevinylene)–poly(amidoamine) (PPV–PAMAM) hybrid dendrimer (Transgeden) that was able to bind and release small interfering ribonucleic acid (siRNA) and lacked any toxicity on neurons at the concentrations used to deliver the genetic cargo.[6] The dendriplexes efficiently engendered a decrease of more than 92% in the expression of specific mRNAs, indicating that Transgeden is a promising nonviral gene delivery carrier and an efficient tool for gene therapy in cerebellar granular neurons and cortical neurons.[6,7] The striking outcomes in gene delivery efficiency produced by small dendrons and dendrimers seem to be intrinsically related to the formation of supramolecular aggregates, although experimental structure-relationship studies are still needed in order to clarify some issues. In addition, these aggregates may be used to stabilize gold nanoparticles, which represent another important class of nanoparticle platforms and a new approach for tagging biologically active macromolecules. Likewise, metallic nanoparticles have proven to be the most flexible nanostructures, together with dendrimers, owing to the synthetic control of their size, shape, composition, structure, assembly, and encapsulation as well as the resulting tunability of their optical properties.[8]

We report here the synthesis and characterization of a PPV–PAMAM hybrid family of dendrimers from first to third

Received: July 17, 2013
Revised: August 25, 2013
Published: September 6, 2013

Scheme 1. Preparation of the PPV–PAMAM Hybrid Dendrimers (TGD G*n*)

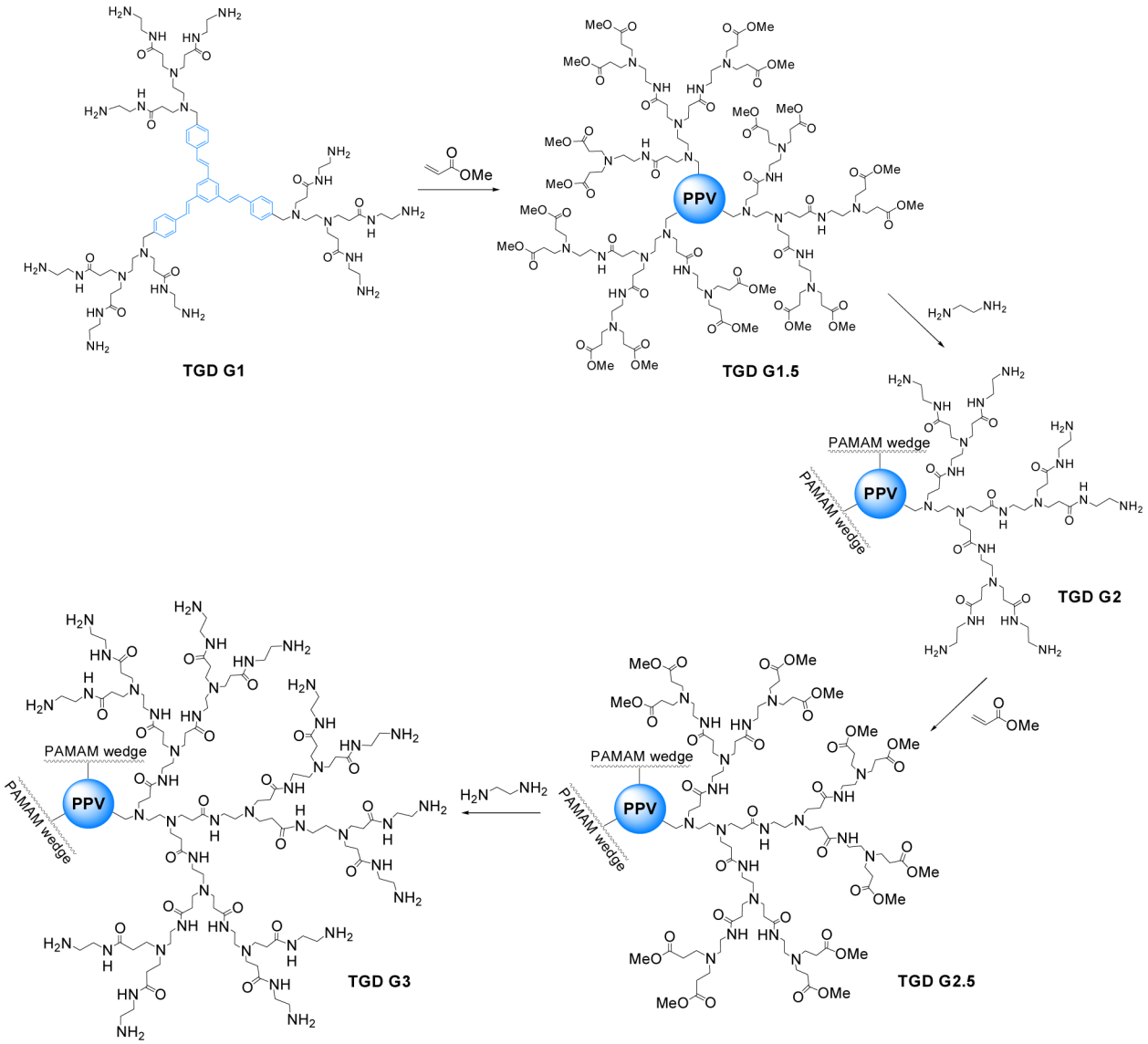

generation as well as a complete study of their aggregation based on different techniques such as encapsulation of Nile Red and dynamic light scattering (DLS). We also present the optimized conditions to prepare different sizes of gold nanoparticles stabilized by these dendrimers in order to combine the aforementioned attributes of Transgeden with the unique properties of gold nanoparticles that make them useful as biomarkers in living whole cells.[8,9] The characterization of these systems and their influence on the optical properties of the supramolecular structures are discussed.

EXPERIMENTAL SECTION

Compound TGD G1.5. To a cooled solution (ice bath) of dendrimer **TGD G1** (122 mg, 0.075 mmol) in anhydrous methanol (20 mL) was added dropwise methyl acrylate (0.185 mL, 2.04 mmol) under an argon atmosphere. The mixture was stirred at room temperature for 48 h in the absence of light. The solvent and excess methyl acrylate were removed under vacuum (temperature <40 °C). A further purification was performed by addition of dry methanol (3 × 10 mL) and subsequent evaporation to give 235 mg (yield >99%) of **TGD G1.5** as a yellowish oil. ^{1}H NMR ($CDCl_3$, 500 MHz) δ: 2.34–2.64 (m, 84H, 42 × CH_2), 2.73–2.88 (m, 54H, 27 × CH_2), 3.24–3.30 (m, 18H, 9 × C$\underline{H}_2$NHCO), 3.64 (s, 6H, 3 × CH_2Ar), 3.66 (s, 18H, 6 × OCH_3), 3.67 (s, 36H, 12 × OCH_3), 7.08 (broad, NH), 7.12 (broad, NH), 7.14 (A of AB_q, 3H, J = 16.5 Hz, 3 × CH═), 7.20 (B of AB_q, 3H, J = 16.5 Hz, 3 × CH═), 7.31 (A of AB_q, 6H, J = 8.5 Hz, ArH), 7.49 (B of AB_q, 6H, J = 8.5 Hz, ArH), 7.55 (s, 3H, ArH), 7.67 (broad, NH). ^{13}C NMR and DEPT ($CDCl_3$, 125 MHz) δ: 173.0 (CO), 172.9 (CO), 172.2 (CO), 172.1 (CO), 138.9 (C), 138.1 (C), 136.0 (C), 129.2 (CH), 128.9 (CH), 128.0 (CH), 126.5 (CH), 123.8 (CH), 58.5 (CH_2), 52.9 (CH_2), 52.2 (CH_2), 51.6 (OCH_3), 51.5 (OCH_3), 51.2 (CH_2), 50.3 (CH_2), 50.0 (CH_2), 49.7 (CH_2), 49.3 (CH_2), 44.6 (CH_2), 37.2 (CH_2), 37.1 (CH_2), 34.0 (CH_2), 33.7 (CH_2), 32.7 (CH_2), 32.6 (CH_2). IR ν: 1730 (C═O) cm^{-1}. MALDI-TOF (THAP) m/z: 3198.6 $[M + Na]^+$, 2281.4 [tropylium cation + $Na]^+$. MALDI-TOF (DHB + 1% TFA) m/z: 919.7 [PAMAM wedge + $2H]^+$ (benzylic fragmentation).

Compound TGD G2.[10] A solution of **TGD G1.5** (235 mg, 0.074 mmol) in ethylenediamine (5 mL, 74 mmol) was stirred for 72 h at room temperature in the absence of light. The solvent was evaporated under vacuum (temperature <40 °C), and the excess ethylenediamine was removed using an azeotropic mixture of toluene:methanol (9:1, 10 mL, three times). The remaining toluene was removed by azeotropic distillation using methanol (10 mL). A further purification was performed by dissolving the oil in dry methanol and using lyophilization to remove the solvent (−80 °C, 0.06 mbar) to give

dx.doi.org/10.1021/ma401505k | *Macromolecules* 2013, 46, 7316–7324

270 mg (>99%) of a yellowish oil. ^{1}H NMR (500 MHz, CD_3OD) δ: 2.30−2.48 (m, 54H, 27 × CH_2), 2.52−2.60 (m, 30H, 15 × CH_2), 2.67−2.90 (m, 90H, 45 × CH_2), 3.20−3.30 (m, 54H, 27 × C$\underline{H}_2$NHCO), 3.67 (broad s, 6H, 3 × CH_2Ar), 7.26 (A of AB_q, 3H, J = 16.0 Hz, 3 × CH═), 7.35 (B of AB_q, 3H, J = 16.0 Hz, 3 × CH═), 7.38 (A of AB_q, 6H, J = 7.5 Hz, ArH), 7.60 (B of AB_q, 6H, J = 7.5 Hz, ArH), 7.70 (s, 3H, ArH), 8.09 (broad, NH). ^{13}C NMR and DEPT (125 MHz, CD_3OD) δ: 175.3 (CO), 175.1 (CO), 174.9 (CO), 174.8 (CO), 140.3 (C), 139.7 (C), 137.8 (C), 130.6 (CH), 130.2 (CH), 129.3 (CH), 127.7 (CH), 125.0 (CH), 59.5 (CH_2), 53.5 (CH_2), 52.4 (CH_2), 52.3 (CH_2), 51.6 (CH_2), 51.3 (CH_2), 51.2 (CH_2), 51.2 (CH_2), 46.4 (CH_2), 43.1 (CH_2), 42.1 (CH_2), 41.7 (CH_2), 39.9 (CH_2), 38.7 (CH_2), 38.7 (CH_2), 36.6 (CH_2), 34.8 (CH_2), 34.7 (CH_2), 34.5 (CH_2). IR ν: 3269 (broad, NH_2), 1643, 1631, 1556 cm^{-1}. MALDI-TOF (DHB + 1% TFA) m/z: 1087.9 $[PAMAM\ wedge + 2H]^+$ (benzylic fragmentation).

Compound TGD G2.5. This compound was prepared from dendrimer **TGD G2** (301 mg, 0.082 mmol) and methyl acrylate (0.396 mL, 4.41 mmol) using the same procedure as described for **TGD G1.5**. After 72 h of reaction, 556 mg (yield >99%) of **TGD G2.5** was obtained as a yellowish-greenish oil. ^{1}H NMR ($CDCl_3$, 500 MHz) δ: 2.36−2.60 (m, 192H, 96 × CH_2), 2.72−2.84 (m, 126H, 63 × CH_2), 3.24−3.30 (m, 54H, 27 × C$\underline{H}_2$NHCO), 3.65 (s, 6H, 3 × CH_2Ar), 3.66 (s, 36H, 12 × OCH_3), 3.67 (s, 72H, 24 × OCH_3), 7.03 (broad, NH), 7.08 (broad, NH), 7.14 (A of AB_q, 3H, J = 16.0 Hz, 3 × CH═), 7.20 (B of AB_q, 3H, J = 16.0 Hz, 3 × CH═), 7.31 (A of AB_q, 6H, J = 8.0 Hz, ArH), 7.50 (B of AB_q, 6H, J = 8.0 Hz, ArH), 7.57 (s, 3H, ArH), 7.76 (broad, NH). ^{13}C NMR and DEPT ($CDCl_3$, 125 MHz) δ: 172.9 (CO), 172.9 (CO), 172.8 (CO), 172.2 (CO), 139.0 (C), 138.0 (C), 135.9 (C), 129.2 (CH), 129.0 (CH), 127.9 (CH), 126.4 (CH), 123.8 (CH), 58.3 (CH_2), 52.9 (CH_2), 52.4 (CH_2), 52.2 (CH_2), 51.5 (OCH_3), 51.4 (OCH_3), 50.3 (CH_2), 50.1 (CH_2), 49.8 (CH_2), 49.7 (CH_2), 49.6 (CH_2), 49.4 (CH_2), 49.2 (CH_2), 49.2 (CH_2), 37.4 (CH_2), 37.1 (CH_2), 37.0 (CH_2), 33.9 (CH_2), 33.8 (CH_2), 32.6 (CH_2), 32.6 (CH_2), 32.5 (CH_2). IR ν: 1730 (C═O) cm^{-1}.

Compound TGD G3. This compound was prepared from dendrimer **TGD G2.5** (556 mg, 0.082 mmol) and ethylenediamine (5 mL, 74 mmol) using the same procedure as described for **TGD G2**. After 72 h of reaction, 639 mg (>99%) of **TGD G3** was obtained as a yellowish-greenish oil. ^{1}H NMR (500 MHz, CD_3OD) δ: 2.32−2.43 (m, 126H, 63 × CH_2), 2.54−2.87 (m, 264H, 132 × CH_2), 3.23−3.26 (m, 126H, 63 × C$\underline{H}_2$NHCO), 3.68 (broad s, 6H, 3 × $ArCH_2$), 7.27 (A of AB_q, 3H, J = 16.0 Hz, 3 × CH═), 7.37 (B of AB_q, 3H, J = 16.5 Hz, 3 × CH═), 7.38 (A of AB_q, 6H, J = 8.0 Hz, ArH), 7.60 (B of AB_q, 6H, J = 8.0 Hz, ArH), 7.72 (s, 3H, ArH), 8.10 (broad, NH). ^{13}C NMR and DEPT (125 MHz, CD_3OD) δ: 175.2 (CO), 175.1 (CO), 175.0 (CO), 174.9 (CO), 174.7 (CO), 174.6 (CO), 140.3 (C), 139.7 (C), 137.7 (C), 130.6 (CH), 130.2 (CH), 129.3 (CH), 127.7 (CH), 125.0 (CH), 53.7 (CH_2), 53.5 (CH_2), 52.4 (CH_2), 51.3 (CH_2), 51.2 (CH_2), 50.9 (CH_2), 47.7 (CH_2), 46.6 (CH_2), 46.5 (CH_2), 46.4 (CH_2), 43.1 (CH_2), 43.0 (CH_2), 43.0 (CH_2), 42.0 (CH_2), 42.0 (CH_2), 41.7 (CH_2), 40.0 (CH_2), 38.6 (CH_2), 36.7 (CH_2), 36.6 (CH_2), 36.5 (CH_2), 34.8 (CH_2), 34.7 (CH_2), 34.6 (CH_2). IR ν: 3280 (NH_2), 1633, 1548 cm^{-1}.

Synthesis of Dendrimer-Stabilized Gold Nanoparticles TGD-(Au^0). 20 mL of a 0.5 mM solution of **TGD-(Au^0)** in Milli-Q water was prepared according to the following method, which is similar to that reported by Crooks and co-workers.[11] Specifically, known volumes (see Supporting Information, Table S1) of a freshly prepared 10.0 mM Milli-Q water solution of $HAuCl_4$ were added to 1 mL of a 10 mM Milli-Q water solution of **TGD G1**. This resulted in NH_3^+:Au^{3+} ratios of 10:1, 25:1, 50:1, and 75:1. The metal−dendrimer complex solution was stirred for less than 1 min, and a 5-fold molar excess (known volume, see Table S1) of a freshly prepared 1 M solution of $NaBH_4$ in 0.3 M NaOH was added. In this way, the final concentration of dendrimer was always 0.5 mM. The vial was then sealed. Reduction occurred almost immediately and was accompanied by a change in color from pale yellow to wine red (see Figure S7). After reduction the mixture was stirred for 1 h and then kept on the bench for 1 day to observe the presence of precipitate. Finally, the solution was dialyzed against Milli-Q water for 2 days (four replacements of water during this time).

RESULTS AND DISCUSSION

Synthesis and Characterization of PPV−PAMAM Hybrid Dendrimers (TGD G*n*). The synthesis of the first generation dendrimer, **TGD G1** (Transgeden), was previously reported by us[6] and starts from a PPV trialdehyde core[12] that provides a unique class of π-conjugated building blocks with optical absorption and emission properties. Following the well-defined synthetic route to PAMAM dendrimers (Michael addition and amidation),[13] second- and third-generation hybrid dendrimers as well as intermediate generations were synthesized (Scheme 1). All compounds were initially obtained as viscous oils, although some of them solidified upon standing or by washing with a solvent such as THF. The presence of the amine groups as peripheral functionalization significantly lowered the solubility of these systems. The materials were sparingly soluble in most of the common solvents when freshly prepared and were even less soluble after solidification, a phenomenon that is probably due to the high tendency of this kind of compound to aggregate. In contrast, the intermediate generations with ester groups at the periphery showed good solubility in chlorinated solvents such as chloroform or dichloromethane.

All new dendrimers were characterized by a variety of analytical techniques. NMR experiments proved very useful to confirm the structures of the compounds (see Figures S1−S4). The *trans* stereochemistry of the double bonds located at the core was preserved throughout the synthetic methodology. This stereochemistry was unequivocally established on the basis of the coupling constant for the vinylic protons in the ^{1}H NMR spectra ($J \approx 16$ Hz). Intermediate generations gave rise to the typical signals attributed to the methyl ester moieties (3.6−3.7 ppm in ^{1}H NMR; 51−52 and 172−173 ppm in ^{13}C NMR), but for **TGD G2** and **TGD G3** these signals were absent. The most characteristic signals for dendrimers **TGD G2** and **TGD G3** in the ^{13}C NMR spectrum corresponded to the amide groups at ∼175 ppm. Overall, all the NMR spectra showed common features for all compounds, with an aromatic region for the conjugated PPV core and an aliphatic region for the PAMAM branches. The broadness of the signals was highly dependent on the deuterated solvent used for the analysis, an observation that indicates high levels of inter- and intramolecular interactions.

As far as the FTIR spectra are concerned, the most important band for intermediate generations, **TGD 1.5** and **TGD 2.5**, is the ester carbonyl stretching at 1730 cm^{-1}. For **TGD G2** and **TGD G3**, the corresponding carbonyl bands are shifted to 1630−1640 cm^{-1}.

Although MALDI-TOF mass spectrometry analyses could be performed using THAP as the matrix, the use of DHB with the addition of 1% of trifluoroacetic acid led to cleaner spectra. In all cases, the experimental results are in good agreement with the expected molecular weights for the different structures, with the spectra all showing a similar pattern. The mass spectrum of the first-generation dendrimer **TGD G1** (see Figure S5) displayed a peak at m/z 1650.4 that can be assigned to corresponding molecular cation $[M + Na]^+$. However, the intensity of this peak is very low compared to the base peak of the spectrum at m/z 1250.6. This base peak can be assigned to a highly favorable benzylic fragmentation that results in the formation of a tropylium cation (Figure S5). The benzylic

dx.doi.org/10.1021/ma401505k | Macromolecules 2013, 46, 7316−7324

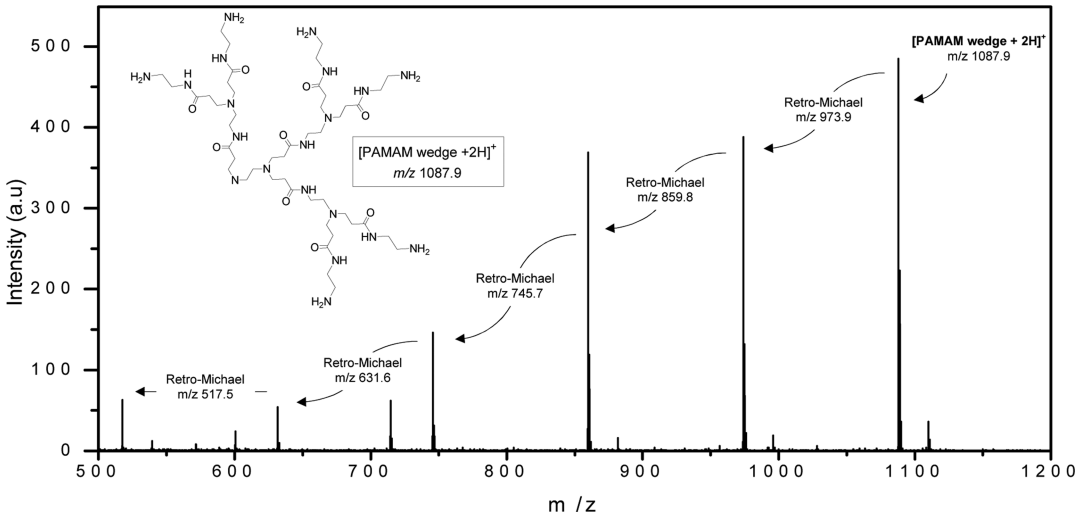

Figure 1. MALDI-TOF mass spectrum of **TGD G2** (matrix: DHB + 1% TFA).

fragmentation was also detected for dendrimers **TGD 1.5** and **TGD 2.0**, and this implies the loss of complete wedges during the analyses. Thus, in the spectrum of **TGD G2** the molecular peak was not observed and the peak corresponding to the PAMAM wedge derived from the benzylic fragmentation was prominent. Furthermore, the addition of strong acid causes the PAMAM wedge to undergo typical retro-Michael reactions leading to a characteristic pattern of fragmentations with several 114.08 m/z losses for this compound (Figure 1). The MALDI-TOF analyses for **TGD 2.5** and **TGD 3.0** gave complex spectra that also contained multiple peaks separated by 114 m/z units, which clearly correspond to successive retro-Michael reactions (see Figure S6).

Finally, it is worth noting that the MALDI-TOF experiments along with the NMR data indicate that, in general, all dendrimers were obtained as almost monodisperse compounds with low levels of molecules with structural defects.

Self-Assembly Studies. Supramolecular self-assembly involves the association of various species to form a larger aggregate and a more complex architecture. In a previous study, we demonstrated the ability of these PPV−PAMAM hybrid dendrimers to self-assemble under different pH and ionic strength conditions.[10] However, a better understanding of the structure of the aggregates is required to provide invaluable structure−activity relationships from which superior hits can be designed and synthesized. Therefore, we were interested in obtaining the critical aggregation concentration (CAC) for all **TGD G*n*** (n = 1−3) molecules.

The method chosen was a Nile Red encapsulation experiment, which has been used by a number of groups to determine the CAC of amphiphiles in aqueous solution.[14] Nile Red is an uncharged heterocyclic molecule, the fluorescence of which varies depending on its surroundings.[15] In a hydrophobic environment, such as the interior of a micelle, Nile Red exhibits high fluorescence at 635 nm, whereas in water the fluorescence output is quenched. Therefore, when mixed with self-assembling vectors, the dye will show enhanced fluorescence when encapsulated within a self-assembled hydrophobic structure, whereas at concentrations below the CAC there will be a significant reduction in fluorescence.

The whole range of fluorescence values against wavelength for each incremental dendrimer concentration for one of the runs is shown in Figure 2 (top) for **TGD G1**. From this graph

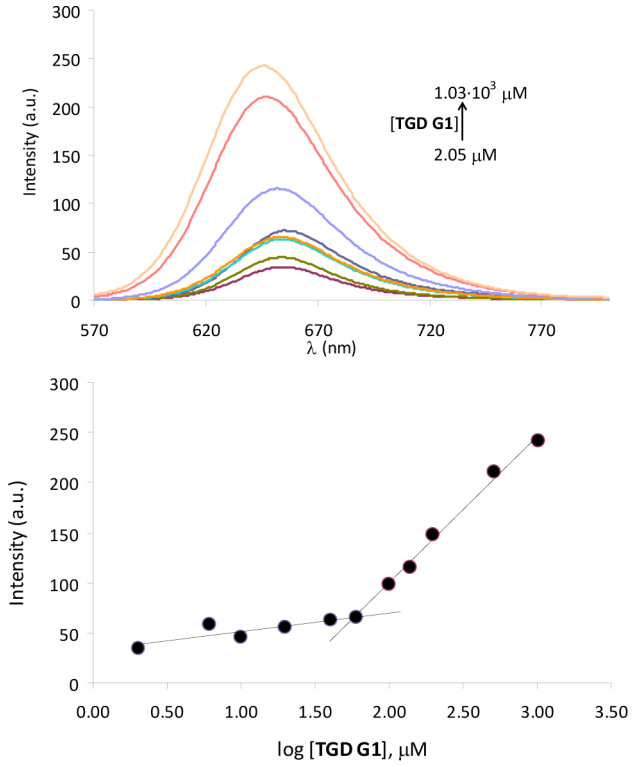

Figure 2. Top: fluorescence spectra (PBS, pH = 7.4) that show an increase in the fluorescence with the corresponding increase in **TGD G1** concentration, thus demonstrating the formation of aggregates. Bottom: fluorescence intensity vs log [**TGD G1**]. The CAC is obtained from the intersection of the two lines.

it is possible to obtain a plot of the log of the concentration of dendrimer against fluorescence intensity, which gives a curve where the point of inflection is equal to the CAC (Figure 2, bottom).[16]

The environment is critical in aggregation phenomena and specific ion effects on the chemical and physical properties of aqueous solutions of synthetic and natural macromolecules are well-known.[17] Hence, the CAC was measured under different conditions. The data obtained confirm that all dendrimers exhibit a high tendency to aggregation, even at relatively low concentrations. **TGD G1** showed a CAC of 9 ± 3 μM in Milli-

dx.doi.org/10.1021/ma401505k | *Macromolecules* 2013, 46, 7316−7324

Q water (pH = 8.2). As expected, a higher ionic strength led to a higher CAC. The use of 10 mM phosphate buffered saline (PBS) at pH = 7.4 resulted in a 6-fold increase in the CAC value (53 ± 4.5 μM), while 5 mM 2-[4-(2 hydroxyethyl)-piperazin-1-yl)ethanesulfonic acid buffer (HEPES buffer) led to a 16-fold increase (144 ± 21 μM at pH = 7.4 and 146 ± 34 μM at pH = 5.5). This higher increase in the CAC value for HEPES is as a consequence of a specific ion effect, since zwitterionic sulfate buffers are known as chaotropic agents (in contrast to kosmotropic agents),[18] i.e., monovalent ions of low charge density that weakly bind water molecules and raise the solubility of proteins and macromolecules.[19]

The generation of the dendrimer is also critical in order to tune the aggregation properties. The CAC for **TGD G2** dropped to 17 ± 12 μM in PBS (pH = 7.4). An increase in the generation resulted in a 3-fold decrease in the CAC value, probably because of the higher number of hydrogen bonds formed, which drive the self-assembly to be more thermodynamically favored and means that this phenomenon takes place at lower concentration. When **TGD G3** was used, fluorescence was not observed at any concentration. It is likely that the bigger PAMAM wedges of this dendrimer inhibit the formation of a micelle with a hydrophobic inner region, and this leads to quenching of the Nile Red fluorescence. Nevertheless, the self-assembly of **TGD G3** was certainly established by dynamic light scattering (DLS) (*vide infra*). Therefore, the main conclusion that can be drawn from these experiments is that **TGD G1** and **TGD G2** form micelle-like aggregates with a nonpolar inner region, probably stabilized through $\pi-\pi$ interactions, and a polar outer region where hydrogen bonding sustains the structure. For **TGD G3**, $\pi-\pi$ interactions are minimized, and only hydrogen bonds are responsible for the aggregates, thus making it difficult to generate hydrophobic regions.

The sizes of the aggregates for all the dendrimers were evaluated by DLS at a concentration higher than the CAC, i.e., 1 mM in PBS (Table 1). The values ranged from 48 ± 10 to 83 ± 24 nm, and the supramolecular structures formed were stable over days. Compared to the sizes previously reported by us for **TGD G1** and **TGD G2** in HEPES,[10] the sizes of the aggregates formed in PBS are slightly smaller. Once again, the chaotropic effect of HEPES facilitates the formation of larger and more polydisperse aggregates for **TGD G1** (75 ± 27 nm) and **TGD G2** (91 ± 31 nm), whereas the kosmotropic effect of PBS results in smaller and less polydisperse aggregates. **TGD G3** forms larger aggregates in comparison to lower generation dendrimers, probably due to the loss of the inner balance interactions between hydrophobic and hydrophilic regions.

Table 1. DLS, Zeta Potentials (ζ), Size Distribution for Gold Nanoparticles, and Fluorescence Quantum Yields of TGD G*n* and TGD-(Au^0)

compound	DLS (nm)	ζ^a (mV)	size^b (nm)	Φ_F
TGD G1	54 ± 6^c			
TGD G2	48 ± 10^c			
TGD G3	83 ± 24^c			
TGD G1^d	57 ± 12	+39 ± 8		0.21
TGD-(Au)^0 10:1^e	8 ± 2	+23 ± 5	3.7 ± 0.9	0.03
TGD-(Au)^0 25:1^e	11 ± 2	+27 ± 5	3.2 ± 0.9	0.02
TGD-(Au)^0 50:1^e	86 ± 15	+34 ± 7	3.5 ± 0.8	0.03
TGD-(Au)^0 75:1^e	79 ± 21	+33 ± 6	2.3 ± 0.4	0.02

^{a}Performed after dialysis at pH ~ 7.5–8.2. ^{b}Size of the gold nanoparticles obtained by TEM. ^{c}In solution of 138 mM NaCl, 2.7 mM KCl and 10 mM PBS. ^{d}Measurements performed after reduction at pH ~ 10. ^{e}NH_3^+:Au^{3+} ratio.

Preparation and Characterization of Dendrimer-Stabilized Gold Nanoparticles. As far as the aggregation results are concerned, PPV–PAMAM hybrid dendrimers can be used to stabilize gold nanoparticles within the interior of the supramolecular aggregates. Typically, the preparation of dendrimer-stabilized gold nanoparticles, **TGD-(Au^0)**, involves the electrostatic complexation of a gold salt ($HAuCl_4$) with the peripheral protonated amino groups of the dendrimer followed by chemical reduction ($NaBH_4$). The dendrimer, in our case **TGD G1**, behaves as surfactant and prevents coalescence and aggregation, and its concentration was always higher than the CAC (Scheme 2). It is well established that the size of the dendrimer-stabilized gold nanoparticles is mainly dependent on the molar ratio between dendrimer and gold atoms.[20] Taking the terminal animo groups of **TGD G1** as a reference, only those with NH_3^+:Au^{3+} ratios of 10:1, 25:1, 50:1, and 75:1 yielded gold nanoparticles [**TGD-(Au^0)**] that were sufficiently stable to be studied. When the NH_3^+:Au^{3+} ratio was lower than 10:1, the dendrimers were not able to stabilize the nanoparticles and precipitation was quickly observed after reduction with $NaBH_4$. In the aforementioned ratios, the gold nanoparticle solutions were stable for several weeks (see Figure S7).

It was possible to tune the average sizes of the gold nanoparticles by controlling the dendrimer-to-$HAuCl_4$ ratio (Table 1). Thus, highly monodisperse spherical-shaped gold nanoparticles with a size of around 3.5 nm were obtained for NH_3^+:Au^{3+} ratios up to 50:1 (Table 1 and Figure 3). However, an increase in this ratio caused a reduction in the nanoparticle size. The electrostatic interaction between the positively charged dendrimers and tetrachloroaurate anions provides a template prior to the nanoparticle formation; a higher amount of dendrimer unequivocally leads to a decrease in the local gold concentration, and this, in turn, leads to a smaller size when the nanoparticles are formed.

When PAMAM dendrimers are used as templates, the dendrimer-stabilized nanoparticles are often larger than 5 nm.[21] The smaller sizes observed with **TGD G1** seem to indicate that the PPV core should play an important role in the stabilization of the nanoparticle and consequently in the final size.

In all cases, under the reaction conditions used (concentration of dendrimer always higher than the CAC) the gold nanoparticles must be surrounded by multiple molecules as we depict in Scheme 2. **TGD G1** is a low-generation dendrimer, and its limited terminal amines and open structure cannot entrap a metal nanoparticle within the interior.

The behavior shown by **TGD G1** and **TGD-(Au^0)** in solution is very important to answer two main questions. The first concerns the size and charge that these nanostructures have in solution because these features will determine the biological performance of the systems. The second question to be answered concerns how the gold nanoparticle affects the nature of the **TGD G1** aggregates. In an effort to answer these questions, DLS and zeta potential (ζ) experiments were performed.

DLS showed that the sizes of all **TGD-(Au^0)** particles were rather different to those of the **TGD G1** aggregates (57 nm, Table 1). Higher quantities of gold result in smaller aggregates (8–11 nm), and a decrease in the amount of gold increases the size of the aggregates (79–86 nm). The incorporation of the gold nanoparticle should disturb the interactions between

dx.doi.org/10.1021/ma401505k | *Macromolecules* 2013, 46, 7316–7324

Scheme 2. Preparation of Gold Nanoparticles Stabilized by TGD G1 Molecules

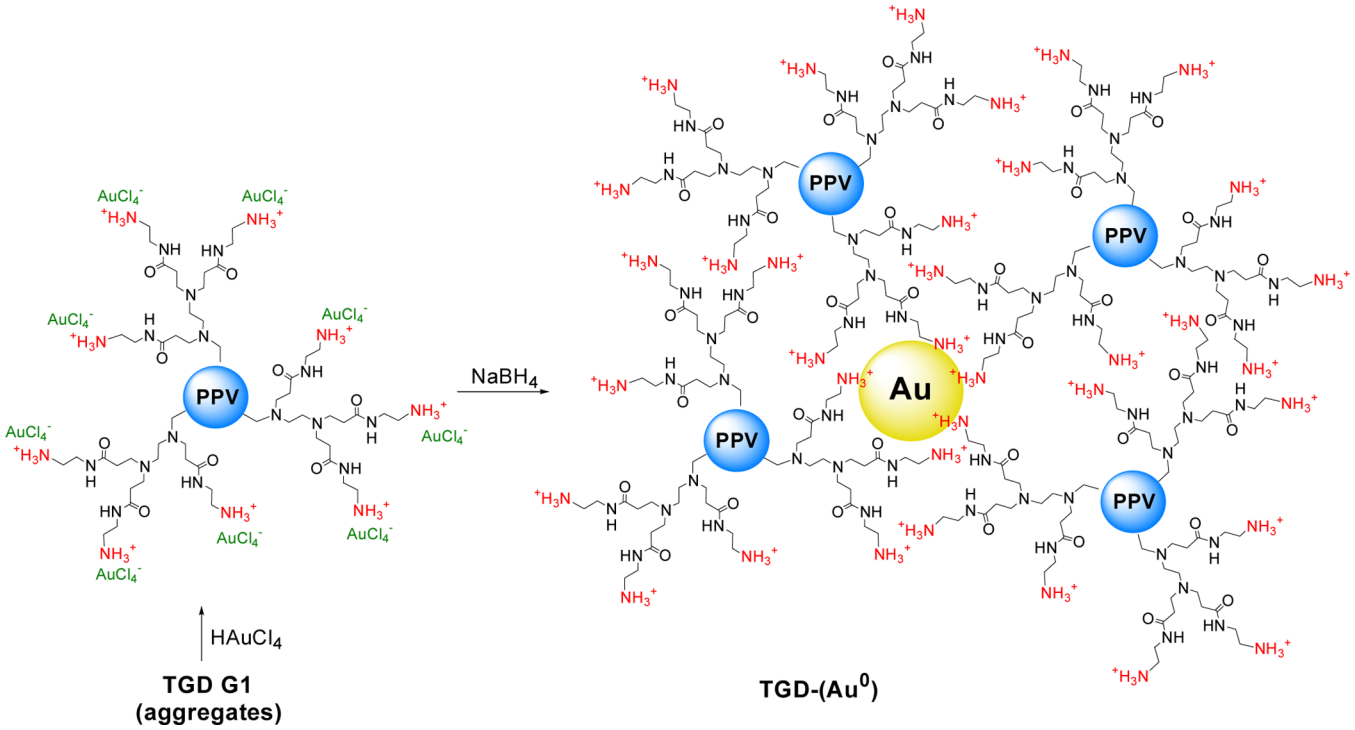

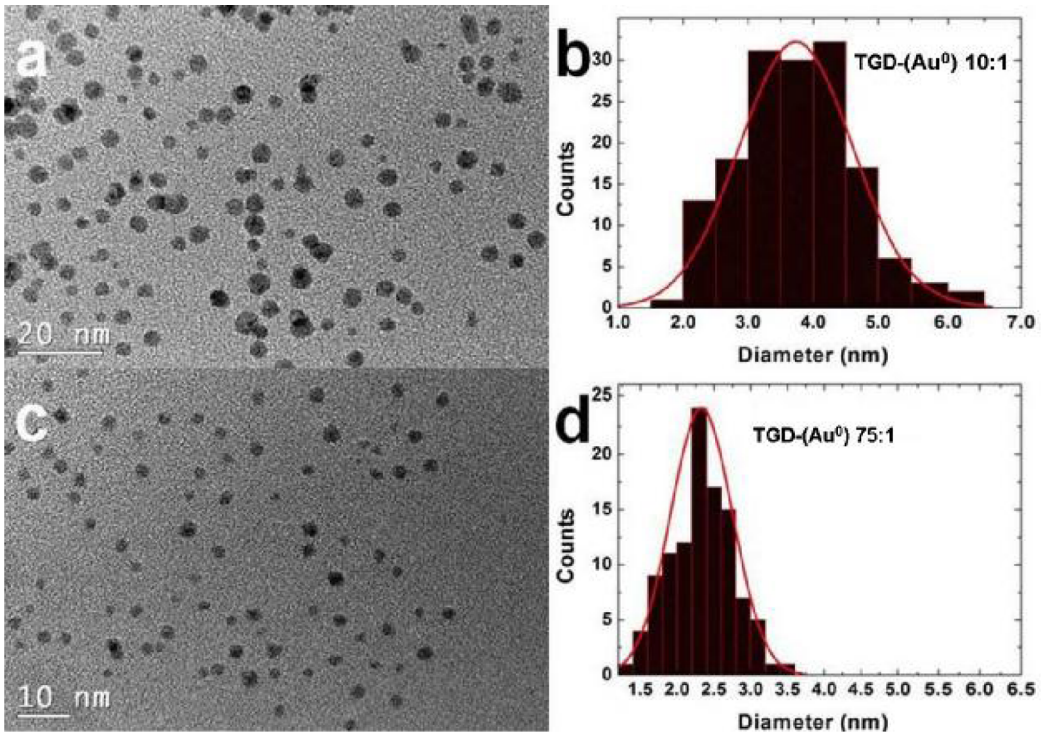

Figure 3. (a) TEM image of a **TGD-(Au^0) 10:1** sample and (b) the corresponding histogram. (c) TEM image of a **TGD-(Au^0) 75:1** sample and (d) the corresponding histogram.

dendrimer molecules, and this would affect the self-assembly process.

On the other hand, zeta potential measurements (ζ) proved that all the **TGD-(Au^0)** systems were positively charged (Table 1), with ζ values ranging from +20 to +40 mV at pH = 7.5−8.2. These results indicate that after the formation of the gold nanoparticles the terminal amines of the dendrimer are still available to be protonated.[22] The cationic charge density and the steric effect of **TGD-G1** keep the nanoparticles apart and lead to stable colloids. As expected, ζ measurements also confirmed that a higher level of gold leads to a lower positive charge in the bulk solution, probably due to the interaction between amino groups and gold nanoparticles. Dialyzed solutions with less gold have a potential of around +30−40

dx.doi.org/10.1021/ma401505k | *Macromolecules* 2013, 46, 7316−7324

mV, which is similar to that of **TGD G1** in the absence of gold (+39 mV). However, solutions with higher levels of gold (NH_3^+:Au^{3+} ratios ranging from 10:1 to 25:1) have ζ values between +23 and +27 mV.

Thermogravimetric analysis (TGA) results for **TGD-G1** and **TGD-(Au^0)** are shown in Figure 4. The weight loss observed

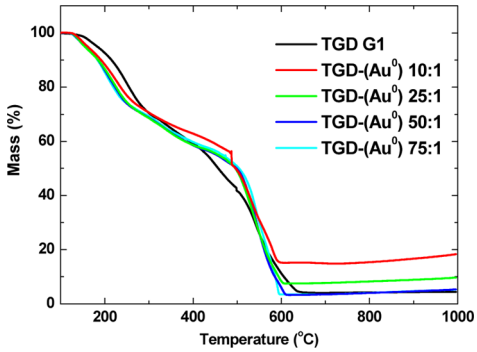

Figure 4. TGA traces for dialyzed samples of **TGD G1** and **TGD-(Au^0).** 5% weight loss temperatures: 183 °C for **TGD G1**, 161 °C for **TGD-(Au^0) 10:1**, 154 °C for **TGD-(Au^0) 25:1**, 155 °C for **TGD-(Au^0) 50:1**, and 156 °C for **TGD-(Au^0) 75:1.** The measurements were performed under an air atmosphere, and the heating rate was 10 °C/min.

for each sample can be attributed to a loss of the dendrimer that stabilizes the gold particle surface. At 700 °C the organic moiety was fully removed. These experiments allowed us to determine the amount of gold that it is retained by the dendrimers after dialysis. Taking into account the molecular weight of **TGD G1** and the atomic weight of gold oxide, it is possible to estimate the amount of gold per dendrimer and compare it to the initial amount of gold added to the solution. In this way, we calculated gold contents of 10.0% for **TGD-(Au^0) 10:1** and 3.2% for **TGD-(Au^0) 25:1**. These values are significantly lower than the quantities of gold initially added to the solution (15.4% and 6.7%, respectively). These results indicate a lack of efficiency of the **TGD G1** molecules to retain all the gold atoms. Analysis of **TGD-(Au^0) 50:1** and **TGD-(Au^0) 75:1** showed that the final amount of gold present was so small that it could not be determined as it fell within the experimental error of the instrument used.

Optical Properties. The hybrid dendrimer **TGD G1** combines, within the same structure, flexible PAMAM branches and a conjugated rigid PPV, which we used as an internal chromophore probe for fluorescence tagging. This material emits blue light when irradiated and shows a typical response in the visible region (λ_{max} = 399 and 413 nm in Milli-Q water). This fluorescence allowed us to detect the presence of the dendrimer within the interior of cells when it operated as gene delivery carrier. Nevertheless, excitation should take place at 319 nm (λ_{max} of absorption), but this is not particularly useful for biological applications because of the harmful effects of UV radiation. For this reason, the presence of gold nanoparticles may be a less damaging alternative for biocompatible tracers.

We also studied the optical properties, UV/vis, and fluorescence of the **TGD-(Au^0)** nanoassemblies in Milli-Q water after dialysis. It is widely known that gold nanoparticles strongly absorb and scatter visible light. The absorption of light energy excites the free electrons in the gold particles to give a collective oscillation, the so-called surface plasmon. The scattered light intensity is extremely sensitive to the size and aggregation state of the particles.[23] The UV/vis spectra of **TGD-(Au^0)** showed a monotonically decreasing absorbance toward higher wavelength and a very small plasmon band at 522 nm (Figure 5a). The broad width and small absorbance of this band suggest that the particles are very small (diameter ~2 nm),[24] which is in agreement with the preceding data obtained by TEM.

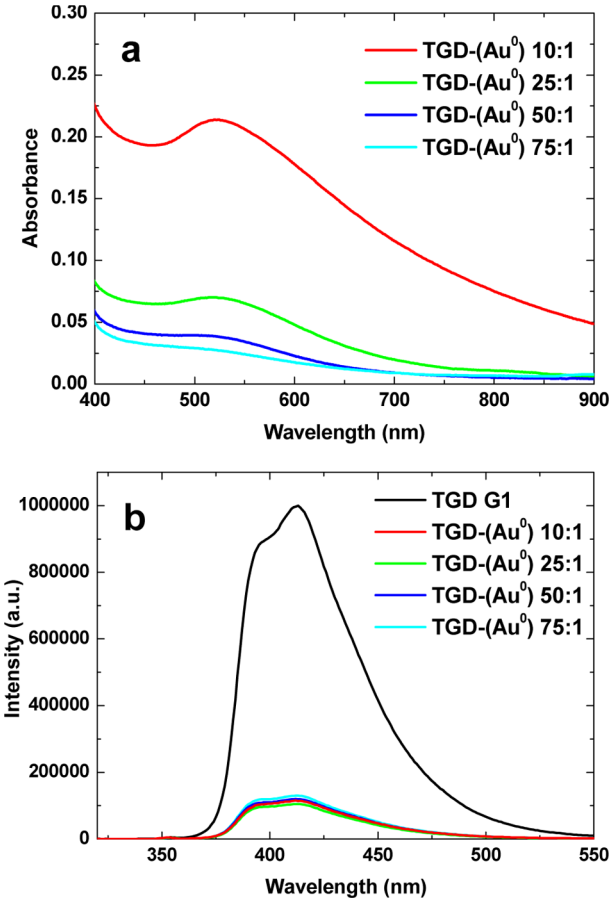

Figure 5. (a) UV/vis spectra of different **TGD-(Au^0)** samples. (b) Fluorescence spectra of **TGD-(Au^0).** All the samples were run after dialysis at c = 20 μM, except for **TGD G1**, which was run at 1.6 μM in Milli-Q water.

Depending on the distance between the fluorescent unit and the gold nanoparticle, the nanoparticle size, and the loading of the fluorescent dye on the nanoparticle, energy transfer may prevent photons from being emitted (or enhance their emission). The fluorescence spectra of different samples of **TGD-(Au^0)** are shown in Figure 5b. A quenching process can clearly be observed regardless of the gold content of the sample. A study of the fluorescence quantum yield renders a series of values that also indicate strong quenching of the fluorescence caused by the presence of gold (Table 1). It is considered that this quenching effect can be attributed to two different causes: (i) the gold nanoparticles increase the nonradiative rate of the molecules due to energy transfer, and (ii) the radiative rate of the molecules is decreased because the molecular dipole and the dipole induced on the nanoparticle radiate out of phase if the molecules are oriented tangentially to the gold surface.[25] Both processes are particle-dependent, and higher quenching efficiencies have been reported to occur with small nanoparticles.[9]

dx.doi.org/10.1021/ma401505k | Macromolecules 2013, 46, 7316−7324

CONCLUSIONS

The synthesis and characterization of a series of PPV−PAMAM hybrid dendrimers, from first to third generation as well as the intermediate generations, are reported. It has been clearly demonstrated that the dendrimers **TGD G*n*** self-assemble into macromolecular structures. The presence of a planar hydrophobic core facilitates the interaction between dendrimer molecules and creates an inner hydrophobic region. A Nile Red encapsulation experiment was used to determine the CAC in different media. DLS measurements complemented the self-assembly study and permitted an evaluation of the size of the aggregates above the CAC. **TGD G1** was used to stabilize gold nanoparticles within the interior of the supramolecular aggregates. TEM and UV/vis indicated that small nanoparticles were always obtained regardless of the NH^{3+}:Au^{3+} ratio used in their synthesis. The nanoparticle showed an important influence on the assembly and the optical properties of the dendrimer and led to strong quenching of the PPV core fluorescence, an observation that indicates the proximity between the gold nanoparticle and the chromophoric moiety of the dendrimer in the aggregates. Importantly, these particles will facilitate the recognition of nanoassemblies in cellular media by means of electron microscopy because of their high electron contrast. Ongoing studies are being carried out in order to shed light on the nature of the entities that deliver the siRNA, to corroborate their internalization into cells, and to provide a structure−activity relationship that will help to explain the biological activity of the PPV−PAMAM hybrid dendrimers.

ASSOCIATED CONTENT

Supporting Information

Experimental methods, details for the preparation of gold nanoparticles, copies of ^{1}H NMR and ^{13}C NMR spectra for all new compounds, and copies of MALDI-TOF mass spectra for **TGD G1** and **TGD G3**. This material is available free of charge via the Internet at http://pubs.acs.org.

AUTHOR INFORMATION

Corresponding Author

*E-mail: julian.rodriguez@uclm.es (J.R.-L.).

Author Contributions

‖J.G. and A.C.R. have contributed equally to this work.

Notes

The authors declare no competing financial interest.

ACKNOWLEDGMENTS

This research was funded by Ministerio de Economía y Competitividad (Spain)/FEDER (EU) (projects BFU2011-30161-C02-01 and 02). V.C. also thanks the support of Junta de Comunidades de Castilla La Mancha (projects PII1I09-0163-4002 and POII10-0274-3182). J.G. and A.C.R. acknowledge the receipt of a Torres Quevedo contract and an FPI fellowship, respectively.

REFERENCES

(1) (a) Salata, O. V. *J. Nanobiotechnol.* **2004**, *2*, 3. (b) Medina, C.; Santos-Martínez, M. J.; Radomski, A.; Corrigan, O. I.; Radomski, M. W. *Br. J. Pharmacol.* **2007**, *150*, 552−558. (c) Pérez-Martínez, F. C.; Posadas, I.; Guerra, J.; Ceña, V. *Pharm. Res.* **2011**, *28*, 1843−1858. (d) Posadas, I.; Guerra, J.; Ceña, V. *Nanomedicine (London, U. K.)* **2010**, *5*, 1219−1236. (e) Mintzer, M. A.; Simanek, E. E. *Chem. Rev.* **2008**, *109*, 259−302.

(2) Faraji, A. H.; Wipf, P. *Bioorg. Med. Chem.* **2009**, *17*, 2950−2962.

(3) (a) Vögtle, F.; Richard, G.; Werner, N. *Dendrimer Chemistry: Concepts, Syntheses, Properties, Applications*; Wiley-VCH: Weinheim, 2009. (b) *Designing Dendrimers*; Campagna, S., Ceroni, P., Puntoriero, F., Eds.; Wiley: New York, 2011. (c) *Dendrimers: Towards Catalytic, Material and Biomedical Uses*; Caminade, A.-M., Turrin, C.-D., Laurent, R., Ouali, A., Delavaux-Nicot, B., Eds.; Wiley: Chichester, 2011.

(4) (a) *Dendrimer-Based Nanomedicine*; Majoros, I. J., Baker, Jr., J. R., Eds.; Pan Stanford Publishing: Singapore, 2008. (b) Boas, U.; Christensen, J. B.; Heegaard, P. M. H. *Dendrimers in Medicine and Biotechnology. New Molecular Tools*; RSC Publishing: Cambridge, 2006. (c) Mignani, S.; El Kazzouli, S.; Bousmina, M.; Majoral, J.-P. *Prog. Polym. Sci.* **2013**, *38*, 993−1008.

(5) (a) Barnard, A.; Posocco, P.; Pricl, S.; Calderon, M.; Haag, R.; Hwang, M. E.; Shum, V. W. T.; Pack, D. W.; Smith, D. K. *J. Am. Chem. Soc.* **2011**, *133*, 20288−20300. (b) Jones, S. P.; Gabrielson, N. P.; Wong, C. H.; Chow, H. F.; Pack, D. W.; Posocco, P.; Fermeglia, M.; Pricl, S.; Smith, D. K. *Mol. Pharmaceutics* **2011**, *8*, 416−429. (c) Wood, K. C.; Azarin, S. M.; Arap, W.; Pasqualini, R.; Langer, R.; Hammond, P. T. *Bioconjugate Chem.* **2008**, *19*, 403−405. (d) Wood, K. C.; Little, S. R.; Langer, R.; Hammond, P. T. *Angew. Chem., Int. Ed.* **2005**, *44*, 6704−6708. (e) Bayele, H. K.; Ramaswamy, C.; Wilderspin, A. F.; Srai, K. S.; Toth, I.; Florence, A. T. *J. Pharm. Sci.* **2006**, *95*, 1227−1237. (f) Al-Jamal, K. T.; Ramaswamy, C.; Florence, A. T. *Adv. Drug Delivery Rev.* **2005**, *57*, 2238−2270. (g) Al-Jamal, K. T.; Ramawamy, C.; Singh, B.; Florence, A. T. *J. Drug Delivery Sci. Technol.* **2005**, *15*, 11−17. (h) Shah, D. S.; Sakthivel, T.; Toth, I.; Florence, A. T.; Wilderspin, A. F. *Int. J. Pharm.* **2000**, *208*, 41−48. (i) Guillot-Nieckowski, M.; Eisler, S.; Diederich, F. *New J. Chem.* **2007**, *31*, 1111−1127. (j) Guillot, M.; Eisler, S.; Weller, K.; Merkle, H. P.; Gallani, J. L.; Diederich, F. *Org. Biomol. Chem.* **2006**, *4*, 766−769. (k) Joester, D.; Losson, M.; Pugin, R.; Heinzelmann, H.; Walter, E.; Merkle, H. P.; Diederich, F. *Angew. Chem., Int. Ed.* **2003**, *42*, 1486−1490.

(6) Rodrigo, A. C.; Rivilla, I.; Pérez-Martínez, F. C.; Monteagudo, S.; Ocaña, V.; Guerra, J.; García-Martínez, J. C.; Merino, S.; Sánchez-Verdú, P.; Ceña, V.; Rodríguez-López, J. *Biomacromolecules* **2011**, *12*, 1205−1213.

(7) (a) Posadas, I.; Pérez-Martínez, F. C.; Guerra, J.; Sánchez-Verdú, P.; Ceña, V. *J. Neurochem.* **2012**, *120*, 515−527. (b) Pérez-Carrión, M. D.; Pérez-Martínez, F. C.; Merino, S.; Sánchez-Verdú, P.; Martínez-Hernández, J.; Luján, R.; Ceña, V. *J. Neurochem.* **2012**, *120*, 259−268. (c) Pérez-Carrión, M. D.; Ceña, V. *Pharm. Res.* **2013**, *30*, 2584−2595.

(8) Giljohann, D. A.; Seferos, D. S.; Daniel, W. L.; Massich, M. D.; Patel, P. C.; Mirkin, C. A. *Angew. Chem., Int. Ed.* **2010**, *49*, 3280−3294.

(9) Saha, K.; Agasti, S. S.; Kim, C.; Li, X.; Rotello, V. M. *Chem. Rev.* **2012**, *112*, 2739−2779.

(10) Pavan, G. M.; Monteagudo, S.; Guerra, J.; Carrión, B.; Ocaña, V.; Rodríguez, F. J.; Danani, A.; Perez-Martinez, F. C.; Ceña, V. *Curr. Med. Chem.* **2012**, *19*, 4929−4941.

(11) (a) García-Martínez, J. C.; Crooks, R. M. *J. Am. Chem. Soc.* **2004**, *126*, 16170−16178. (b) Kim, Y.-G.; Oh, S.-K.; Crooks, R. M. *Chem. Mater.* **2004**, *16*, 167−172.

(12) (a) Garcia-Martínez, J. C.; Diez-Barra, E.; Rodríguez-López, J. *Curr. Org. Synth.* **2008**, *5*, 267−290. (b) Díez-Barra, E.; García-Martínez, J. C.; Merino, S.; del Rey, R.; Rodríguez-López, J.; Sánchez-Verdú, P.; Tejeda, J. *J. Org. Chem.* **2001**, *66*, 5664−5670.

(13) Tomalia, D. A.; Baker, H.; Dewald, J.; Hall, M.; Kallos, G.; Martin, S.; Roeck, J.; Ryder, J.; Smith, P. *Polym. J.* **1985**, *17*, 117−132.

(14) (a) Rodrigo, A. C.; Barnard, A.; Cooper, J.; Smith, D. K. *Angew. Chem., Int. Ed.* **2011**, *50*, 4675−4679. (b) Lim, Y. B.; Lee, E.; Lee, M. *Angew. Chem., Int. Ed.* **2007**, *46*, 9011−9014. (c) Stuart, M. C. A.; van de Pas, J. C.; Engberts, J. *J. Phys. Org. Chem.* **2005**, *18*, 929−934.

(15) Fowler, S. D.; Greenspan, P. *J. Histochem. Cytochem.* **1985**, *33*, 833−936.

(16) Lim, Y. B.; Lee, E.; Lee, M. *Angew. Chem., Int. Ed.* **2007**, *46*, 9011−9014.

(17) (a) Zhang, Y.; Cremer, P. S. *Curr. Opin. Chem. Biol.* **2006**, *10*, 658−663. (b) von Hippel, P. H.; Scheleich, T. *Acc. Chem. Res.* **1969**, *2*, 257−265.
(18) (a) Jensen, W. A.; Armstrong, J. M.; De Giorgio, J.; Hearn, M. T. W. *Biochemistry* **1995**, *34*, 472−480. (b) Wu, C.-F.; Cha, H. J.; Valdes, J. J.; Bentley, W. E. *Biotechnol. Bioeng.* **2002**, *77*, 212−218.
(19) (a) Liu, X.-Y.; Mu, X.-R.; Liu, Y.; Liu, H.-J.; Chen, Y.; Cheng, F.; Jiang, S.-C. *Langmuir* **2012**, *28*, 4867−4876. (b) Leberman, R.; Soper, A. K. *Nature* **1985**, *378*, 364−366.
(20) Esumi, K. *Top. Curr. Chem.* **2003**, *227*, 31−52.
(21) Shen, M.; Shi, X. *Nanoscale* **2010**, *2*, 1596−1610.
(22) Tomalia, D. A.; Naylor, A. M.; Goddard, W. A., III *Angew. Chem., Int. Ed. Engl.* **1990**, *29*, 138−175.
(23) (a) Sokolov, K.; Aaron, J.; Hsu, B.; Nida, D.; Gillanwater, A.; Follen, M.; Macaulay, C.; Adler-Storthz, K.; Korgel, B.; Discour, M.; Pasqualini, R.; Arap, W.; Lam, W.; Richartz-Kortum, R. *Technol. Cancer Res. Treat.* **2003**, *2*, 491−504. (b) Jain, P. K.; Lee, K. S.; El-Sayed, I. H.; El-Sayed, M. A. *J. Phys. Chem. B* **2006**, *110*, 7238−7248. (c) Daniel, M. C.; Astruc, D. *Chem. Rev.* **2003**, *104*, 293−346.
(24) (a) Gröhn, F.; Bauer, B. J.; Akpalu, Y. A.; Jackson, C. L.; Amis, E. J. *Macromolecules* **2000**, *33*, 6042−6050. (b) Torigoe, K.; Suzuki, A.; Esumi, K. *J. Colloid Interface Sci.* **2001**, *241*, 346−356. (c) Kim, Y. G.; García-Martínez, J. C.; Crooks, R. M. *Langmuir* **2005**, *21*, 11981−11986.
(25) Dulkeith, E.; Ringler, M.; Klar, T. A.; Feldmann, J.; Muñoz Javier, A.; Parak, W. J. *Nano Lett.* **2005**, *5*, 585−589.